Atmos. Chem. Phys. Discuss., https://doi.org/10.5194/acp-2019-315
Manuscript under review for journal Atmos. Chem. Phys.
Discussion started: 13 May 2019

Atmospheric Chemistry and Physics Discussions

Is the photochemistry activity weak during haze events? —— A novel exploration on the photoinduced heterogeneous reaction of NO_2 on mineral dust

Tao Wang[1], Yangyang Liu[1], Yue Deng[1], Hanyun Cheng[1], Yang Yang[1], Yiqing Feng[1], Muhammad Ali Tahir [1], Xiaozhong Fang[1], Xu Dong[1], Kejian Li[1], Saira Ajmal[1], Aziz-Ur-Rahim Bacha[1], Iqra Nabi[1], Hongbo Fu[1], Liwu Zhang[1,2*], Jianmin Chen[1]

[1] Shanghai Key Laboratory of Atmospheric Particle Pollution and Prevention, Department of Environmental Science & Engineering, Fudan University, Shanghai, 200433, Peoples' Republic of China

[2] Shanghai Institute of Pollution Control and Ecological Security, Shanghai, 200092, Peoples' Republic of China

Abstract

Despite the increased awareness of heterogeneous reaction on mineral dust, the knowledge of how the intensity of solar irradiation influences the photochemistry activity remains a crucially important part in atmospheric research. Relevant studies have not seriously discussed the photochemistry under weak sunlight during haze, and thus ignored some underlying pollution and toxicity. Here, we investigated the heterogeneous formation of nitrate and nitrite under various illumination conditions by laboratory experiments and field observations. Observed by *in-situ* diffuse reflectance infrared Fourier transform spectroscopy (DRIFTS), water-solvated nitrate was the main surface product, followed by other species varying with illumination condition. The growth of nitrate formation rate tends to be slow after the initial fast with increasing light intensity. For example, the geometric uptake coefficient (γ_{geo}) under 30.5 mW/cm^2 (5.72×10^{-6}) has exceeded the 50 % of that under 160 mW/cm^2 (1.13×10^{-5}). This case can be explained by the excess NO_2 adsorption under weak illumination while the excess photoinduced active species under strong irradiation. Being negatively associated with nitrate (R^2=0.748, P<0.01), nitrite acts as the intermediate and decreases with increasing light intensity via oxidation pathways. Similar negative dependence appears in coarse particles collected during daytime (R^2=0.834, P<0.05), accompanied by the positive association during nighttime (R^2=0.632, P<0.05), suggesting illumination a substantial role in atmospheric nitrogen cycling. Overall, for the nitrate formation, the conspicuous response under slight illumination offers opportunities to explain the secondary aerosol burst during haze episodes with weak irradiation. Additionally, high nitrite levels accompanied by low nitrate concentrations may induce great health risk which was previously neglected. Further, Monte Carlo simulation coupled with sensitivity analysis may provide a new insight in the estimations of kinetics parameters for atmospheric modelling studies.

Atmos. Chem. Phys. Discuss., https://doi.org/10.5194/acp-2019-315
Manuscript under review for journal Atmos. Chem. Phys.
Discussion started: 13 May 2019

Atmospheric Chemistry and Physics Discussions

1 Introduction

Secondary nitrate aerosols, deriving mainly from various oxidation processes of nitrogen oxides, are of great importance in atmospheric chemistry **(Anenberg et al., 2017)**. These ubiquitous species is key for describing the composition and sources of particulate matters **(Huang et al., 2014; Schuttlefield et al., 2008)**. It was investigated that the contributions of nitrate to the particle mass concentration increase throughout the pollution episodes **(Guo et al., 2014)**. However, current atmospheric models fail to capture the serve nitrate enhancement from the clean to haze period, and thus triggers the discussion on the heterogeneous reaction of NO_2 on primary aerosols **(Tan et al., 2016)**. Modeling studies indicated that nitrate formation is highly associated with airborne mineral dust **(Tan et al., 2016)**. Accounting for ~36% of the total primary aerosol emissions, mineral dust is one of the most abundant particle types in the troposphere **(Chen et al., 2012; Usher et al., 2003)**. During their global journey, many heterogeneous reactions take place on the particle surface, and further affect the atmospheric oxidation capacity **(Tang et al., 2017)**. This process has aroused widespread interest in East Asia because dust occupies a great share in fine particles due to the frequent occurrence of sand storms **(Zhang et al., 2015)**. Hence, the heterogeneous reaction of NO_2 on mineral dust is worthy of broader concerns.

Titanium dioxide (TiO_2) is found in mineral dust at mass mixing ratios ranging from 0.1% to 10% depending on the exact location from where the particles were uplifted **(Ndour et al., 2008)**. Compared to other non-semiconducting components in mineral dusts, TiO_2 has direct environmental implications for its photocatalysis **(Nanayakkara et al., 2014)**. Prior studies have indicated the photoinduced oxidation of trace gases by TiO_2 an essential role in the chemical balance of the atmosphere **(Chen et al., 2012)**. Additionally, TiO_2-coating surfaces are currently used on building exteriors, road lamps and road bricks **(Ballari et al., 2010; Ballari et al., 2011)**. These self-cleaning materials in populated urban areas facilitate the irreversible removal of NO_2 from atmosphere with the substantial formation of gaseous nitrous acid (HONO) and ozone **(Balajka et al., 2018; Langridge et al., 2009; Monge et al., 2010)**. Accordingly, TiO_2 is frequently adopted as the reference material on behalf of the ubiquitous semiconducting components in atmospheric environment, especially the urban atmosphere.

For the heterogeneous process on mineral dust, prior studies put close attention to varied influential factors. Among these, moisture and temperature are widely concerned and significant advances have been made **(Li et al., 2010; Tan et al., 2017; Tan et al., 2016; Wang et al., 2012)**. Although being treated as an important index in many atmospheric discussions, illumination has not been systematically investigated for its effects on the heterogeneous uptake of trace gases. Most remarkable studies concerned the photocatalytic effects instead of the

Atmos. Chem. Phys. Discuss., https://doi.org/10.5194/acp-2019-315
Manuscript under review for journal Atmos. Chem. Phys.
Discussion started: 13 May 2019

Atmospheric Chemistry and Physics Discussions

dependence on illumination conditions **(Dupart et al., 2014; Guan et al., 2014)**. Some researchers **(El Zein and Bedjanian, 2012)** measured the reactive uptake coefficients (γ-values) for the heterogeneous reaction of NO_2 on TiO_2 under various irradiance intensities while ignored the reaction mechanism behind the variation. Furthermore, nitrite is of great significance in atmospheric processes for its frequent appearance and great contributions to aerosol toxicity. However, there is little information available in literature about the pollution characteristics or reaction pathways of nitrite aerosols. Generally, how the illumination influences the uptake capacity and product species are problems urgently needs solving.

This work aims to provide a fresh perspective to explore the light dependence for the heterogeneous reaction on mineral dust. Monte Carlo simulation is introduced to evaluate the kinetics for nitrate formation. Atmospheric particulates were collected and analyzed to support relevant findings. This research could help further understand the illumination effects in the atmospheric nitrogen cycling, and simultaneously provide extremely valid parameters for modelling studies.

2 Experimental

2.1 Materials

Commercial TiO_2 (Degussa, Germany), with an anatase-to-rutile ratio of 3: 1, an average particle size of 12.05±3.46 nm and a Brunauer-Emmett-Teller (BET) specific surface area (S_{BET}) of 55.83±0.35 $m^2 \cdot g^{-1}$ was employed as the photocatalytic mineral dust ***(SI, Section S1)***. All chemicals were of analytical grade and obtained from Aladdin Chemical Reagent Co., Ltd. Water in all experiments was ultrapure water (specific resistance ≧ 18.2 MΩ cm).

High-pure air (79% N_2 and 21% O_2, Shanghai TOMOE Co., LTD, China) and 300 parts per million (ppm) NO_2 (N_2 dilution, Shanghai Qingkuan Co., LTD, China) were included in this research. Prior to coming into the gas supply system, high-pure air went through silica gel and molecular sieve for drying and purification.

2.2 DRIFTS experiments

A FTIR spectrometer (Tracer-100, Shimadzu, Japan) equipped with a liquid-nitrogen-cooled mercury-cadmium-telluride (MCT) detector was applied to record in situ DRIFTS spectra with 100 scans averaged for each spectrum and a resolution of 4 cm^{-1}. We have described the general features of the setup in ***Figure S2*** and previous reports **(Wang et al., 2018a; Wang et al., 2018b; Wang et al., 2018c)**. Herein, a xenon lamp (CEL-TCX250, Beijing Ceaulight Co., LTD, China) was used to provide simulated solar irradiation upon the particles ***(Figure S3)***.

Prior to each experiment, the particles were pretreated in a stream of high-pure air (200 ml·min^{-1}) for 60 min to remove the adsorbed water and impurities from the surfaces ***(Figure S4)***. Due to the overlapping bands of adsorbed water (~1640 cm^{-1}) and nitrogen compounds, the sample after pretreatment was exposed to humid high-pure air (RH≈30%, 100 ml·min^{-1}) for 20 min, after which the moisture absorption reaches saturation ***(Figure S5)***. A background spectrum was recorded after the process and then NO_2 calibration gas (5.12 ml·min^{-1}) was added into the DRIFTS chamber with a calculated concentration of 15.33 ppm. Calibration gases with NO_2 concentrations of 9.20 and 21.45 ppm were also involved for the concentration dependence experiments. Ten light intensity levels (0.0, 0.3, 5.4, 17.5, 23.8, 30.5, 54.5, 98.5, 128.1, and 160.0 mW·cm^{-2}) were referred in this study.

Each test lasted 90 min, during which a series of spectra were recorded every 5 min. The reacted particles were extracted by oscillation (5 min) with 4 ml water. The extraction solution was then passed through a 0.22 μm PTFE membrane filter for ion detection.

2.3 Ion analysis

The nitrate and nitrite ions were analyzed by an ion chromatography (IC, 883 Basic, Metrohm, Switzerland), which consists of an analytical column (A5-250) and a guard column. The detection was conducted by using 3.2 mmol·L^{-1} Na_2CO_3 and 1.0 mmol·L^{-1} $NaHCO_3$ at a stable flow rate of 0.70 ml·min^{-1}. Multipoint calibrations were performed by means of standard solutions. Good linearity of the calibration curve was obtained with R^2>0.998.

2.4 Photo-electrochemical (PEC) test

In order to qualitatively evaluate the generation of electron-hole pairs under different light intensities, PEC tests were conducted by a electrochemical workstation (CHI-660D, Shanghai Chenhua Co., LTD, China) in a three-electrode cell with a quartz window **(Yang et al., 2017; Zheng et al., 2015)**. TiO_2 particles were deposited on a sheet of fluorine-tin-oxide glass to serve as the working electrode with an effective area of 1cm^2. A platinum wire and an Ag/AgCl electrode were employed as the counter and reference electrodes, respectively. The electrolyte was 0.5 mol/L $NaNO_3$. A xenon lamp (CEL-S500, Beijing Ceaulight Co., LTD, China) was used to provide simulated sunlight.

2.5 Uptake coefficient estimation

The reactive uptake coefficient, γ, is defined as the ratio of the reactive gas-surface collision rate ($d[NO_3^-]/dt$) to the total gas-surface collision rate (Z) **(Gustafsson et al., 2006)**. The equations are shown as follows.

$$\gamma = \frac{d[NO_3^-]/dt}{Z} \qquad Eq.(1)$$

$$\frac{d[NO_3^-]}{dt} = slope \times f \qquad Eq.(2)$$

$$Z = \frac{1}{4} \times A_S \times [NO_2] \times v_{NO_2} \qquad Eq.(3)$$

$$v_{NO_2} = \sqrt{\frac{8RT}{\pi M_{NO_2}}} \qquad Eq.(4)$$

Where *slope* represents the growth rate of the nitrate peaks, *f* is the conversion factor, A_s is the particle reactive surface area, v_{NO_2} is the mean velocity of NO_2 molecule, [NO_2] is the NO_2 concentration, *R* is the gas constant, T is the temperature, M_{NO_2} is molecular weight of NO_2 ***(Table S1)***.

The conversion factor (*f*) is obtained from a calibration plot with the amount of NO_3^- versus the integrated areas for nitrate **(Tan et al., 2017; Tan et al., 2016)**. The factor is $2.09\times10^{15}\pm1.61\times10^{14}$ (ion · K-M unit^{-1}) in this study ***(Figure S6)***. For the A_s, both geometric surface area (A_{geo}) and BET surface area (A_{BET}) are mentioned to evaluate the upper and lower limits of the γ-values (denoted as γ_{geo} and γ_{BET}, respectively) varying with reaction probabilities between reactants and particles.

Monte Carlo simulation was implemented to deal with the uncertainties **(Chiang et al., 2009; Ginsberg and Belleggia, 2017; Xia et al., 2013)**. Each independent variable was determined via five or more replication measurements and assumed to be normally distributed in the simulation. Based on earlier finds, 5000 iterations are sufficient to ensure the stability of the results. Additionally, sensitivity analysis is helpful in exploring the variables that influence the estimation most. Pearson correlation coefficients between each variable and the output (γ-value) were calculated and then normalized to 100%. On this basis, the contribution of each input variable to the output can be assessed. Three input variables are included for γ_{geo}: *slope*, *f*, and A_s. For γ_{BET}, the A_s is further divided into mass and S_{BET} as discussed above.

2.6 Particle sampling and chemical analysis

Aerosols were collected in the late summer and early autumn in the campus of Fudan University, Shanghai, China ***(Figure S8)***. The first stage from 23th August to 17th September contains 26 daily samples. The second stage lasted from 21th to 29th September, including eight sample sets collected during daytime and another eight during nighttime.

The size-segregated samples ranging from 0.4 to 100 μm were collected on quartz fiber filters (Whatman, UK) using an eight stage micro-orifice uniform deposit impactor (Anderson, Tisch Environmental Inc, USA) operating at a flow rate of 28.3 L/min. The particle modes were defined as follows: 0-0.56 μm for condensation mode, 0.56-1.8 μm for droplet mode, and 1.8-100 μm for coarse mode.

Before sampling, the filters were pre-combusted at 550℃ for 4 h to minimize original impurities. After collection, the filters were extracted ultrasonically by 20 ml water for 45 min. Water extracts were passed through a 0.22 μm PTFE membrane filter for NO_3^- and NO_2^- detection as introduced in **section 2.3**.

3 Results and discussion

3.1 Observed species on particles

Figure 1 presents the DRIFTS spectra recorded in the absence and presence of illumination, coupled with the Gaussian curve-fitting procedure to deconvolute the overlapping bands. The fitting was undertaken until reproducible results were obtained with the coefficient of determination (R^2) greater than 0.990. The bands in the spectra are quite rich, indicating various products as summarized in ***Table S3***.

Under illumination, the signals peaking at 1312 and 1553 cm^{-1} reflect the formation of monodentate nitrate, whereas those at 1276, 1573, and 1602 cm^{-1} account for the vibration of bidentate nitrate **(Figure 1d, e) (Li et al., 2010; Ma et al., 2011; Niu et al., 2017; Szanyi et al., 2007)**. Bridging bidentate nitrate can be further identified by the shoulder peak at 1602 cm^{-1} **(Du et al., 2019; Goodman et al., 1998; Sun et al., 2016)**. Besides, the peaks at 1347 and 1412 cm^{-1} are assigned to water-solvated nitrate **(Baltrusaitis et al., 2007; Guan et al., 2014; Miller and Grassian, 1998)**. Under dark condition, except the similar bands appearing under illumination (1561, 1409, 1323, and 1271 cm^{-1}), some nitrite products become more attractive as evident by the monodentate nitrite at 1195 and 1440 cm^{-1}, as well as the bidentate nitrite around 1308 cm^{-1} **(Figure 1a, b) (Wu et al., 2013)**. Water-solvated nitrate is far ahead in amount compared to other species **(Figure 1c, f)**, suggesting weak links between the products and particle surfaces. Hence, the surface water layers of the hygroscopic particles provides plenty active space for the heterogeneous uptake of NO_2.

After the reversible adsorption of NO_2 on mineral dust ***(R.S1)***, the NO_2 reacts with hydroxyl-related groups (OH^-) or surface H_2O to form adsorbed nitrate/nitrite or free nitric acid/nitrous acid, respectively ***(R.S2-S3)***. Since no acid molecules were observed, free nitrite and nitrate ions stem from ionization ***(R.S4-S5)***. The disproportionation process ***(R.1)*** dominates the dark reaction. When excited with light (wavelength≥390 nm), there is the generation of electron-hole pairs in the conduction and valence bands of TiO_2 ***(R.S6)*** **(Dupart et al., 2014; FUJISHIMA and HONDA, 1972; Yu and Jang, 2018)**. Photogenerated holes and electrons react with H_2O and O_2, and thus lead to the formation of hydroxyl radicals ($OH^{\cdot}$) and reactive oxygen radicals ($O_2^{\cdot-}$), respectively ***(R.S7-S8)*** **(Chen et al., 2012)**. Superoxide hydrogen radical ($HO_2^{\cdot}$) and hydrogen peroxide (H_2O_2) appear and produce $OH^{\cdot}$ as well ***(R.S7-S14)***. These photoinduced active species (PAS) would accelerate the nitrate formation ***(R.2)***.

Atmos. Chem. Phys. Discuss., https://doi.org/10.5194/acp-2019-315
Manuscript under review for journal Atmos. Chem. Phys.
Discussion started: 13 May 2019

Atmospheric Chemistry and Physics Discussions

176 $$NO_2 \xrightarrow{OH^-/H_2O} NO_3^- + NO_2^- \quad R.(1)$$

177 $$NO_2 \xrightarrow{h\nu \ \& \ TiO_2} NO_3^- \quad R.(2)$$

178 Noticeably, nitrite (especially monodentate type) decreases in proportion as the dark reaction proceeds,
179 accompanied by the increasing contribution from bidentate nitrate species and water-solvated ones ***(Figure 1c,***
180 ***S10a)***. The nitrite would react with another surface nitrite in a Langmuir-Hinshelwood mechanism ***(R.3)*** or
181 gaseous NO_2 in an Eley-Rideal mechanism ***(R.4)*** to form nitrate in the absence of illumination **(Tang et al., 2018;**
182 **Underwood et al., 1999)**. Oxygen also acts as a promoter in the nitrite oxidation **(Tang et al., 2018)**. On the other
183 hand, diverse nitrate species make steady contributions to the total products during the photoreactions ***(Figure***
184 ***S10b)***. Generally, nitrite signal is visible in dark, while gradually fades away after irradiation due to the oxidation
185 of nitrite to nitrate by PAS via ***R.5 (Section S8)***.

186 $$2NO_2^- \rightarrow NO_3^- + NO + e^- \quad R.(3)$$

187 $$NO_2^- + NO_2 \rightarrow NO_3^- + NO \quad R.(4)$$

188 $$NO_2^- \xrightarrow{h\nu \ \& \ TiO_2} NO_3^- \quad R.(5)$$

189 Illumination has impacts on either product species or the production. The final DRIFTS spectra grow in
190 intensity as the illumination becomes stronger. Raman measurements also indicate the drastic enhancement caused
191 by sunlight, evident by the higher nitrate peak after illumination compared to that after dark process ***(Section S9)***
192 **(Fu et al., 2017; Yu et al., 2018; Zhao et al., 2018)**. These observations provide a solid evidence that the nitrate
193 formation on mineral dust is enhanced under sunlight, in nice agreement with previous results **(Dupart et al.,**
194 **2014; Guan et al., 2014)**. Noticeably, the nitrate determined by IC exhibits a clear nonlinear uptrend with
195 increasing light intensity, suggesting uneven illumination effect on nitrate formation **(Figure 1g)**. On the contrary,
196 the nitrite presents a nonlinear downtrend **(Figure 1h)**, and thus results in the negative association with nitrate
197 **(Figure 1i)**. What is the proposed mechanism behind the uneven illumination effects? Whether the photoinduced
198 negative dependence appears in atmospheric particulates? We may discuss these issues in the following sections.

Atmos. Chem. Phys. Discuss., https://doi.org/10.5194/acp-2019-315
Manuscript under review for journal Atmos. Chem. Phys.
Discussion started: 13 May 2019

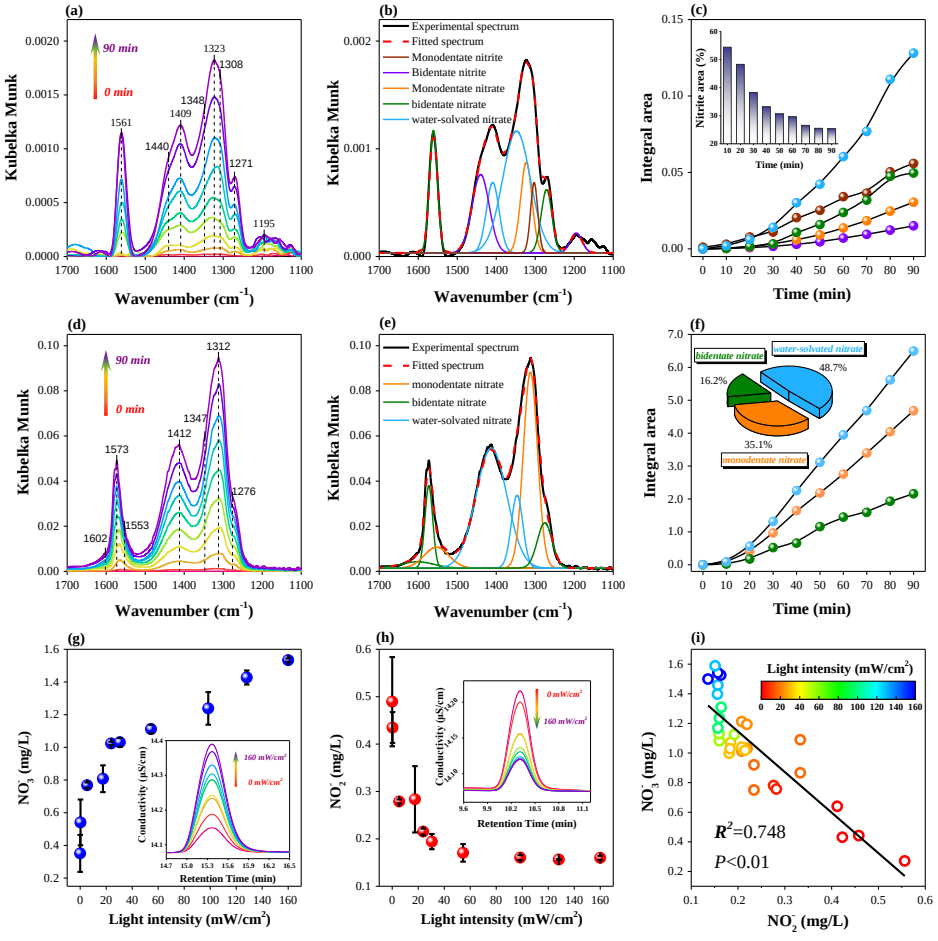

Figure 1. Product observations under **(a-c)** dark condition and **(d-f)** illumination (I=98.5 mW/cm^2), as well as **(g-i)** ion analysis results. **(a, d)** DRIFTS spectra of nitrate and nitrate species. **(b, e)** Peak fitting for the final spectra based on Gaussian method. **(c, f)** Integral areas of diverse species as a function of reaction time. IC measurements for **(g)** nitrate and **(h)** nitrite ions after DRIFTS tests. Error bars represent 1σ. **(i)** Linear association between nitrate and nitrite varying with light intensity. Inset: **(c)** Time-dependent contributions of nitrite, **(f)** Contributions of diverse products after 90 min exposure. **(g, h)** Conductivity spectra from IC.

3.2 Photoinduced uptake capacity

To accurately evaluate the photoinduced nitrate formation, γ-values were estimated based on Monte Carlo simulation with the cumulative probability distributions depicted in **Figure 2** and the percentile values summarized in ***Table S2***. γ_{BET} and γ_{geo} exhibit similar variation trends. Since the reaction is first order with respect

to NO_2 concentration under various light intensities ***(Figure S7)***, the γ-values would still be authentic for atmospheric reactions with lower NO_2 concentrations. The growth of γ-values appears to be slow after the initial fast with increasing light intensity. For instance, the γ_{geo} under 30.5 mW/cm^2 exceeds the half of that under 160 mW/cm^2. To facilitate comparison, theoretical γ-values were calculated in a linear way based on the results under 0 and 160 mW·cm^{-2}. The actual γ-values under 5.4, 17.5, 23.8, 30.5, 54.5, 98.5, and 128.1 mW·cm^{-2} are 73%, 135%, 189%, 158%, 148%, 103%, 39%, and 16% higher than the corresponding theoretical ones, respectively. This 'fast-slow' uptrend seems to be of great importance as it shows that the γ-values measured at designed irradiation intensity may not be extrapolated in a linear way to those relevant to the atmosphere. The balance between PAS formation and NO_2 adsorption is responsible for the uneven illumination effect, which will be carefully discussed in the mechanism section.

To distinguish the contributions of each variable to the output, sensitivity analysis is performed on the basis of the simulated data. Slope and *f* contribute most to the total variance of γ_{BET} and γ_{geo}, while S_{BET} and m for γ_{BET}, and A_{geo} for γ_{geo} contribute little ***(Section S10)***. Accordingly, slope and *f* values in a more accurate level are beneficial for γ-value estimation. More attention in the future needs to be devoted to the stability of DRIFTS and IC measurements.

In view of the great significance of γ_{geo} in atmospheric models, regression analysis is employed to fit the obtained results and further predict values for relevant reactions. Since the γ-values exhibit a 'fast-slow' uptrend, a polynomial regression model ***(Eq.5)*** is used to describe the variation.

$$\gamma_{f,geo} = aI^3 + bI^2 + cI + d \qquad Eq.(5)$$

Where $\gamma_{f,geo}$ is the fitted γ_{geo}, I is light intensity, and a, b, c and d are essential parameters. The final formula ***(Eq.6)*** could explain 99.8% variation of the experimental γ_{geo}, indicating accurate regression **(Figure 2c)**. Furthermore, the $d\gamma_{geo}/dI$ values are obtained by derivation to distinguish the illumination effect varying with light intensity. The uptake capacity is extremely sensitive to light under low intensity, while tends to be light-independent under strong irradiation **(Figure 2d)**. In Shanghai, the 3h-average intensities are mostly lower than 80 mW/cm^2 (NOAA data, https://www.arl.noaa.gov/), indicating noticeable sunlight impacts. More importantly, the irradiation tends to be weaker in winter, highlighting the central role of light-dependent heterogeneous reaction in haze events during cold time.

$$\gamma_{f,geo} = 5.62 \times 10^{-12} \times I^3 - 1.92 \times 10^{-9} \times I^2 + 2.32 \times 10^{-7} \times I + 2.93 \times 10^{-7} \qquad Eq.(6)$$

$$d\gamma_{geo}/dI = 1.686 \times 10^{-11} \times I^2 - 3.84 \times 10^{-9} \times I + 2.32 \times 10^{-7} \qquad Eq.(7)$$

Atmos. Chem. Phys. Discuss., https://doi.org/10.5194/acp-2019-315
Manuscript under review for journal Atmos. Chem. Phys.
Discussion started: 13 May 2019

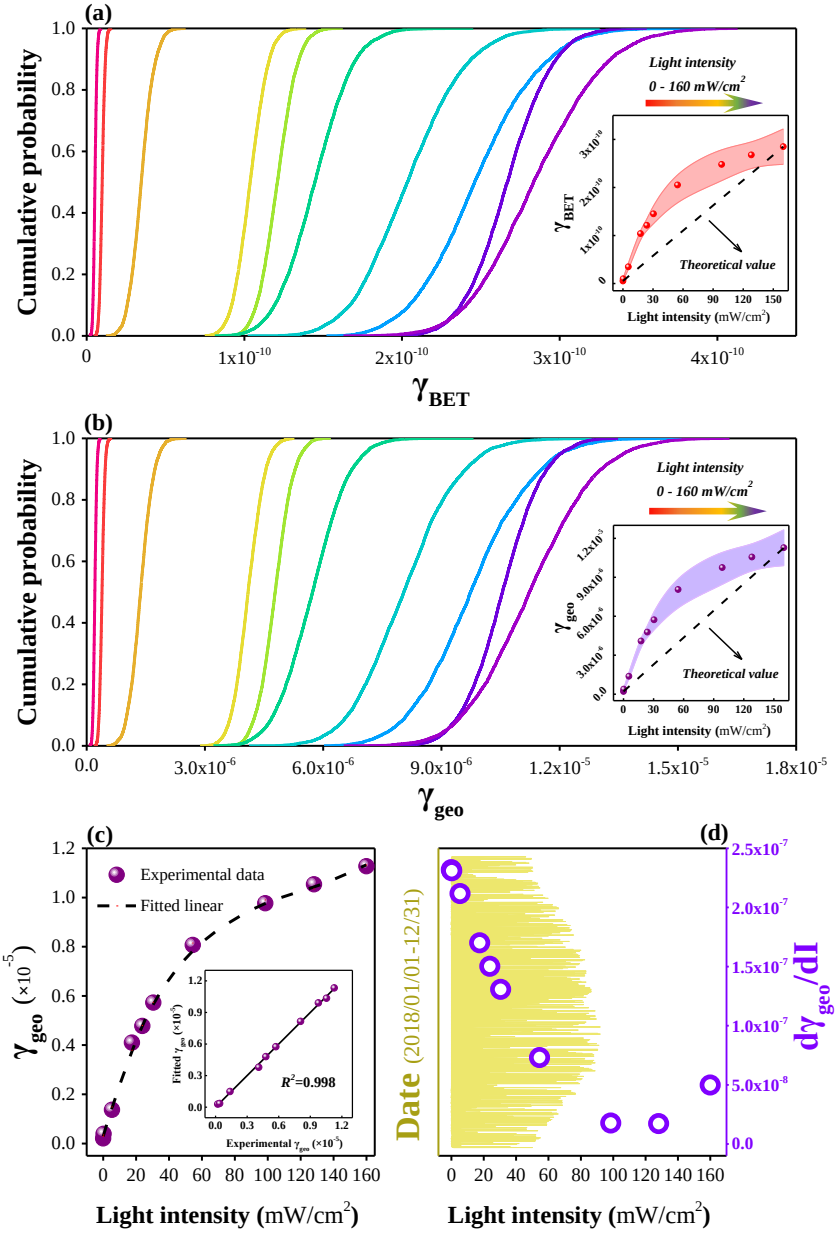

Figure 2. Cumulative probability distribution of the **(a)** γ_{BET} and **(b)** γ_{geo} values based on Monte Carlo simulation. Insets reveal the actual γ-values (Mean±1σ) and theoretical ones. **(c)** Regression analysis on γ_{geo}. Inset presents the linear relation between calculated and fitted values. **(d)** Downward short wave radiation flux (DSWF) in Shanghai, China coupled with estimated $d\gamma_{geo}/dI$.

Atmos. Chem. Phys. Discuss., https://doi.org/10.5194/acp-2019-315
Manuscript under review for journal Atmos. Chem. Phys.
Discussion started: 13 May 2019

Atmospheric Chemistry and Physics Discussions

3.3 Nitrogen redox

Figure 3 presents the association between atmospheric nitrate and nitrite varying with particle mode and sampling period. Significant positive correlation can be found during nighttime in coarse mode **(Figure 3a)**. However, there is no case indicating high nitrite and nitrate levels during daytime, and the dependence seems to be negative **(Figure 3b)**. The correlation turns to be significant with the ignorance of cases where the nitrite and nitrate concentrations are extremely low. As summarized in **section 3.1**, the associations during nighttime and daytime can be explained by the NO_2 disproportionation in the absence of sunlight ***(R.1)*** and the nitrite oxidation under illumination ***(R.5)***, respectively. Daily nitrite and nitrate concentrations exhibit the similar variation with that during daytime, and a negative correlation can be observed based on the classification of nitrite levels **(Figure 3c)**. Noticeably, low nitrite levels are usually accompanied by slight nitrate pollution in the presence of sunlight, resulting mainly from the HONO formation in acidic media ***(R.6)*** **(Liu et al., 2015; Su et al., 2011; Wang et al., 2015; Zhang et al., 2012)** and the photolysis of particulate nitrate ***(R.7)*** **(Nanayakkara et al., 2014; Ostaszewski et al., 2018; Schuttlefield et al., 2008; Ye et al., 2017; Ye et al., 2016)**.

$$NO_2^- + H^+ \leftrightharpoons HNO_2 \leftrightharpoons HONO \qquad R.(6)$$

$$HNO_3 \overset{h\nu}{\Rightarrow} HONO + NO_x \qquad R.(7)$$

Atmospheric nitrate and nitrite from diverse periods exhibit analogous size distribution: greatest in coarse mode, followed by droplet mode and condensation mode ***(Figure S9)***. Yet, except the large mass fraction in coarse mode, nitrite presents extra peak under 1.8 μm, indicating reaction pathways differing from nitrate formation **(Moore et al., 2004)**. That is, nitrate is difficult to accumulate by aqueous reactions or homogeneous processes while nitrite seems to be easy, which results in the lower correlation coefficients for small size particles **(Figure 3d-i)**. Since the main reaction pathways ***(R.1, 3, 4)*** still take place in aqueous media, and some other oxidants (e.g. H_2O_2, O_3, and Fe^{3+}) would replace the promoting role of semiconductor components in mineral dust under illumination ***(R.2, 5)*** **(Hems et al., 2017; Hou et al., 2017; Xue et al., 2016)**, the correlation in droplet mode appears to be obvious with merely lower coefficients. Furthermore, both ions exhibit great mass fractions (>50%) in coarse mode, making the associations for full-size particles similar with those for coarse aerosols **(Figure 3j-l)**.

Generally, atmospheric nitrite is positively correlated with nitrate during nighttime, whereas presents negative association with nitrate in the presence of irradiation. The dependence is significant in coarse mode while turns to be inconspicuous in droplet mode and condensation mode.

Atmos. Chem. Phys. Discuss., https://doi.org/10.5194/acp-2019-315
Manuscript under review for journal Atmos. Chem. Phys.
Discussion started: 13 May 2019

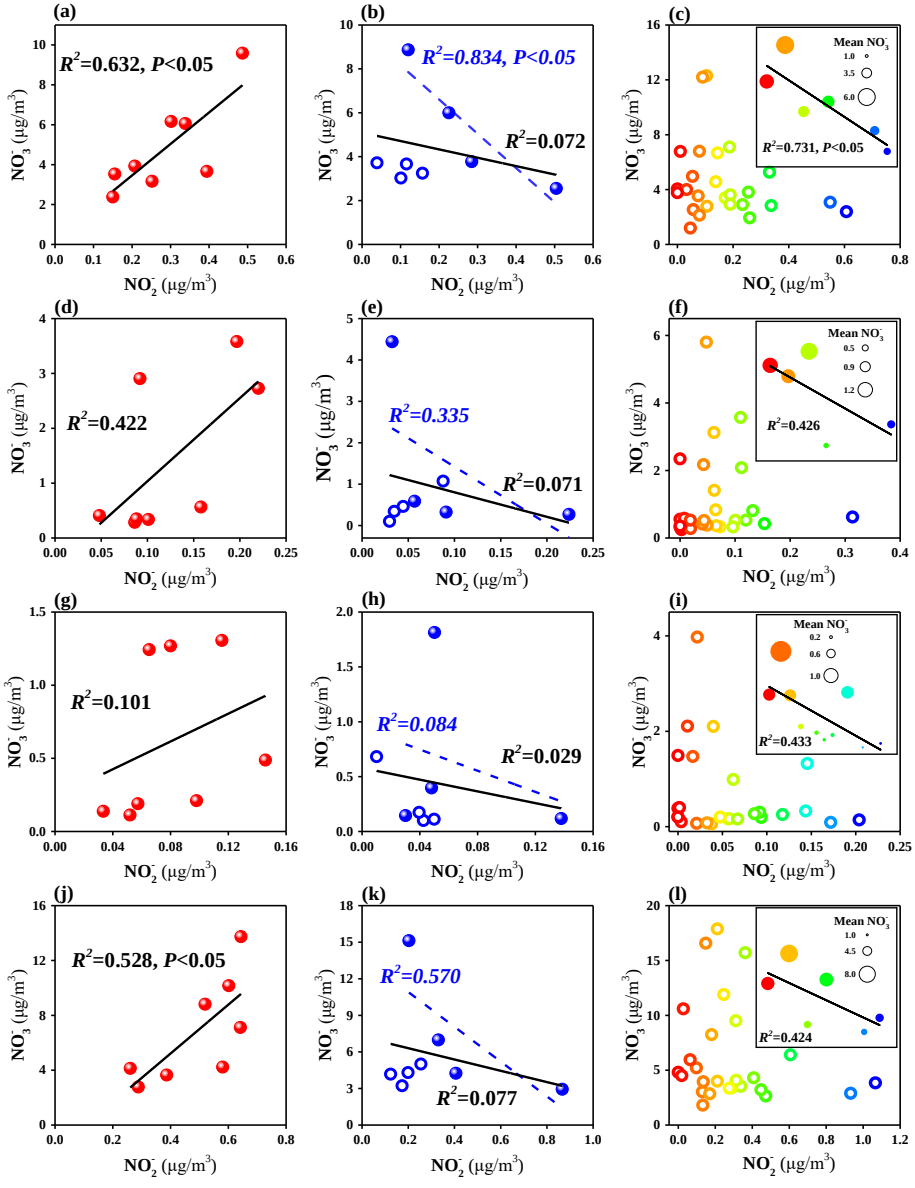

Figure 3. Associations between atmospheric nitrite and nitrate ions in **(a-c)** coarse mode (1.8-100 μm), **(d-f)** droplet mode (0.56-1.8 μm), **(g-i)** condensation mode (0-0.56 μm), and **(j-l)** full-size particles (0-100 μm) collected during **(a, d, g, j)** nighttime, **(b, e, h, k)** daytime, and **(c, f, i, l)** whole day. Insets: mean nitrate concentrations based on nitrite classification. Linear correlation analysis (solid line) was employed for each case. The dashed lines for daytime cases reveal the correlation for solid circles with hollow circles ignored.

Atmos. Chem. Phys. Discuss., https://doi.org/10.5194/acp-2019-315
Manuscript under review for journal Atmos. Chem. Phys.
Discussion started: 13 May 2019

3.4 Mechanism

Main reaction pathways have been introduced in previous sections. However, the uneven illumination effect cannot be explained by chemical equations. The photocurrent of TiO_2 is linearly correlated with light intensity **(Figure 4a)**, indicating even illumination effect on the production of electron-hole pairs. Hence, photocatalytic activity of the mineral dust is not sufficient to explain the uneven nitrate/nitrite formation with illumination variation.

Since no saturation effects were observed in the DRIFTS experiments, the NO_2 adsorption rate can be regarded as constant. Adsorbed NO_2 becomes excess compared to the formed PAS under weak sunlight, and thus makes illumination the rate-limiting factor in oxidation. At this time, nearly all the PAS participate in the oxidation of surface adsorbed NO_2 as well as some nitrite intermediates. When the illumination is strong, the PAS gradually become excess compared to the adsorbed NO_2. Under the circumstances, light makes little contribution to the elevation of uptake capacity and simultaneously NO_2 adsorption turns into the new rate-limiting factor. Generally, it could be deduced that the balance between NO_2 adsorption and PAS formation results in the nonlinear uptrend of γ-values with increasing light intensity.

Concentration dependence was considered in this research, and the nitrate formation rates at given conditions were normalized by the corresponding result estimated at 160 mW/cm^2 **(Figure 4b)**. At low concentration (9.20 ppm), the formation rate is light-dependent under weak illumination while tends to be steady with increasing light intensity, suggesting excess PAS under strong irradiation. The difference is that, at high concentration (21.45 ppm) the formation rate under strong irradiation was not nearly equal to that under 160 mW/cm^2, implying sufficient adsorbed NO_2 at relatively high intensity. Generally, higher NO_2 concentrations suggest broader influence scope of illumination. Hence, current serious NO_2 pollution may increase the participation of solar irradiation in the formation of secondary aerosols.

Atmos. Chem. Phys. Discuss., https://doi.org/10.5194/acp-2019-315
Manuscript under review for journal Atmos. Chem. Phys.
Discussion started: 13 May 2019

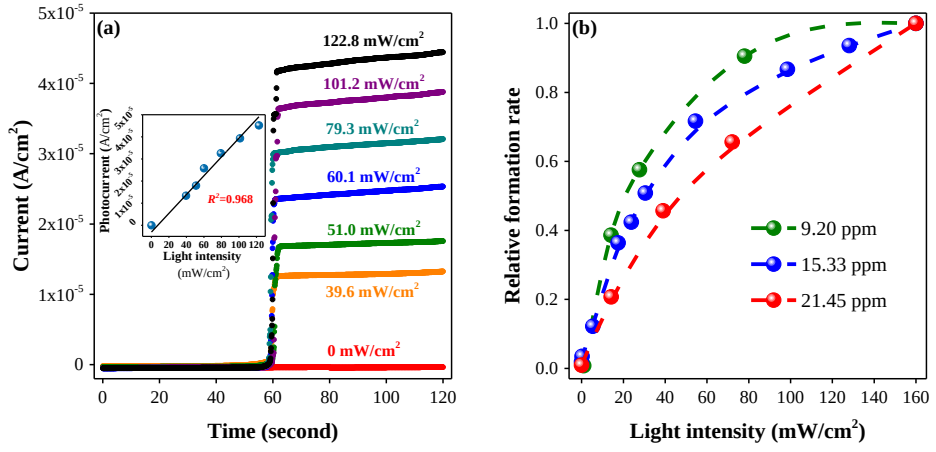

Figure 4. **(a)** Current densities of TiO_2 under various light intensities (60-120 s). Inset: linear correlation between averaged photocurrent densities and irradiation intensities. **(b)** Relative formation rate of nitrate as a function of light intensity under different NO_2 concentrations.

On the other hand, limited PAS participate in the oxidation of excess NO_2 under weak illumination, and thus make space for the nitrite formation via disproportionation process ***(R.1)***. Under strong irradiation, there are still sufficient PAS involved in the nitrite oxidation after the photochemical conversion of limited NO_2 ***(R.2)***. For the oxidation of nitrite intermediates, the main promoters are NO_2 and other nitrite species under dark condition or weak illumination ***(R.3, 4)***, while turns to be PAS under stronger irradiation ***(R.5)***. Hence, nitrite products unevenly decrease with increasing light intensity.

As shown by **Scheme 1**, sunlight influences the formation pathways of nitrate and nitrite aerosols, and finally results in reactions with different features. Mineral dust under weak illumination (or dark condition) and strong irradiation may be covered by different nitrogen compounds: nitrite and nitrate, respectively. Since nitrite may induce cancer risk while nitrate is generally treated as secondary pollutants, we can name them carcinogenic aerosols and polluted aerosols in atmospheric research, respectively.

Atmos. Chem. Phys. Discuss., https://doi.org/10.5194/acp-2019-315
Manuscript under review for journal Atmos. Chem. Phys.
Discussion started: 13 May 2019

Atmospheric Chemistry and Physics Discussions

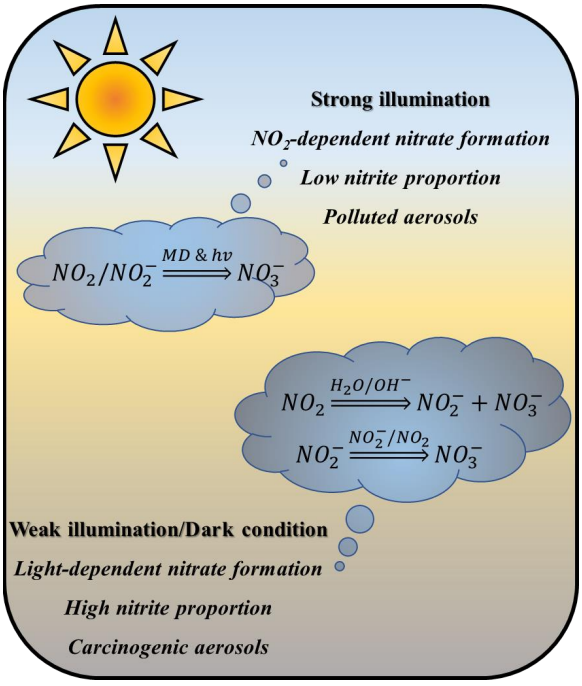

Scheme 1. Characteristics of the photoinduced heterogeneous reaction of NO_2 on mineral dust (MD) under different illumination conditions.

4 Conclusions and atmospheric implications

Nitrate is dominating atmospheric particulates with the increasing NO_x emissions from expanding urban traffic **(Anenberg et al., 2017)**. Photochemistry has traditionally been considered inapparent during haze events because of the weak sunlight near the ground caused by low visibility **(Cheng et al., 2016; Shen et al., 2015; Zhang et al., 2015)**. However, the nitrate formation on mineral dust is found to be more dependent on weak sunlight, indicating that photochemistry processes are still crucial in heavy haze. Since the NO_2 concentrations in the troposphere are much lower than the simulated levels, authentic dust may be close to achieving its highest uptake capacity in the presence of faint sunlight **(Figure 4b)**. Hence, photoinduced reaction on mineral dust may contribute greatly to secondary aerosols during extreme haze events.

Nitrate pollution has got much concern recently, while little attention has been paid to the nitrite burst accompanied by low nitrate concentration. Nitrite may induce adverse health risk for its close association with various cancer cases **(Zhang et al., 2018)**. Compared to the polluted aerosols with high nitrate level, the carcinogenic aerosols with great nitrite concentration may be more harmful to human health. As an intermediate in the photochemistry activities, nitrite appears to be the main product under weak sunlight. The light-dependent

negative correlation between nitrate and nitrite highlights illumination an inducing factor in the atmospheric nitrogen cycling.

Actually, we discussed the γ-values based on the average experimental results while gave little care to various measurement errors. Compared to the arithmetic mean results, the percentile γ-values estimated by Monte Carlo simulation could be more suitable for modelling studies due to the differences between real atmosphere and the simulated laboratory condition. Furthermore, sensitivity analysis is helpful in explaining the determining factors involved in the assessment of uptake capacity. Generally, statistical simulation brings about more accurate evaluation and provides opportunities to explain the model discrepancy for secondary aerosols.

Data availability. All data are available upon request from the corresponding authors.

Supporting information. Sections on particle characterization, experimental setup, pretreatment for in-suit DRIFTS test, uptake coefficient estimation, field observations, product observations, detailed reactions in photocatalytic process, photoinduced nitrite oxidation, Raman detection, Sensitivity analysis.

Author contributions. TW designed the experiments and wrote the paper. YYL and YD contributed to the DRIFTS spectra analysis. YYL and XZF support the field observation. HYC, YQF, MT, and XD assisted the Raman measurements. YY, KJL, SA, AB, and IN performed the PEC tests. LWZ guided the data analysis and paper writing. HBF and JMC provided some experimental facilities. All authors were involved in the discussion.

Competing interests. The authors declare no competing financial interests.

Acknowledgements. The authors gratefully acknowledge financial support from Ministry of Science and Technology of the People's Republic of China (2016YFE0112200, 2016YFC0202700), Marie Skłodowska-Curie Actions (690958-MARSU-RISE-2015), and National Natural Science Foundation of China (21507011, 21677037).

References

Anenberg, S.C., Miller, J., Minjares, R., Du, L., Henze, D.K.: Impacts and mitigation of excess diesel-related NO_x emissions in 11 major vehicle markets, Nature, 545, 467-471, doi: 10.1038/nature22086, 2017.

Balajka, J., Hines, M.A., DeBenedetti, W.J.I., Komora, M., Pavelec, J., Schmid, M., Diebold, U.: High-affinity adsorption leads to molecularly ordered interfaces on TiO_2 in air and solution, Science, 361, 786-789, doi: 10.1126/science.aat6752, 2018.

Ballari, M.M., Hunger, M., Hüsken, G., Brouwers, H.J.H.: NO_x photocatalytic degradation employing concrete pavement containing titanium dioxide, Applied Catalysis B: Environmental, 95, 245-254, doi: 10.1016/j.apcatb.2010.01.002, 2010.

364 Ballari, M.M., Yu, Q.L., Brouwers, H.J.H.: Experimental study of the NO and NO_2 degradation by
365 photocatalytically active concrete, Catal. Today, 161, 175-180, doi: 10.1016/j.cattod.2010.09.028, 2011.
366 Baltrusaitis, J., Schuttlefield, J., Jensen, J.H., Grassian, V.H.: FTIR spectroscopy combined with quantum
367 chemical calculations to investigate adsorbed nitrate on aluminium oxide surfaces in the presence and absence of
368 co-adsorbed water, Phys. Chem. Chem. Phys., 9, 4970-4980, doi: 10.1039/b705189a, 2007.
369 Chen, H., Nanayakkara, C.E., Grassian, V.H.: Titanium dioxide photocatalysis in atmospheric chemistry, Chem.
370 Rev., 112, 5919-5948, doi: 10.1021/cr3002092, 2012.
371 Cheng, Y., Zheng, G., Wei, C., Mu, Q., Zheng, B., Wang, Z., Gao, M., Zhang, Q., He, K., Carmichael, G.,
372 Pöschl, U., Su, H.: Reactive nitrogen chemistry in aerosol water as a source of sulfate during haze events in
373 China, Science Advances, 2, 1-11, doi: 10.1126/sciadv.1601530, 2016.
374 Chiang, K., Chio, C., Chiang, Y., Liao, C.: Assessing hazardous risks of human exposure to temple airborne
375 polycyclic aromatic hydrocarbons, J. Hazard. Mater., 166, 676-685, doi: org/10.1016/j.jhazmat.2008.11.084,
376 2009.
377 Du, C., Kong, L., Zhanzakova, A., Tong, S., Yang, X., Wang, L., Fu, H., Cheng, T., Chen, J., Zhang, S.: Impact
378 of adsorbed nitrate on the heterogeneous conversion of SO_2 on α-Fe_2O_3 in the absence and presence of simulated
379 solar irradiation, Sci. Total Environ., 649, 1393-1402, doi: 10.1016/j.scitotenv.2018.08.295, 2019.
380 Dupart, Y., Fine, L., D'Anna, B., George, C.: Heterogeneous uptake of NO_2 on Arizona Test Dust under UV-A
381 irradiation: An aerosol flow tube study, Aeolian Res., 15, 45-51, doi: org/10.1016/j.aeolia.2013.10.001, 2014.
382 El Zein, A., Bedjanian, Y.: Interaction of NO_2 with TiO_2 surface under UV irradiation: measurements of the
383 uptake coefficient, Atmos. Chem. Phys., 12, 1013-1020, doi: 10.5194/acp-12-1013-2012, 2012.
384 Fu, Y., Kuppe, C., Valev, V.K., Fu, H., Zhang, L., Chen, J.: Surface-Enhanced Raman Spectroscopy: A Facile
385 and Rapid Method for the Chemical Component Study of Individual Atmospheric Aerosol, Environ. Sci.
386 Technol., 51, 6260-6267, doi: 10.1021/acs.est.6b05910, 2017.
387 FUJISHIMA, A., HONDA, K.: Electrochemical Photolysis of Water at a Semiconductor Electrode, Nature, 238,
388 37-38, doi: org/10.1038/238037a0, 1972.
389 Ginsberg, G.L., Belleggia, G.: Use of Monte Carlo analysis in a risk-based prioritization of toxic constituents in
390 house dust, Environ. Int., 109, 101-113, doi: 10.1016/j.envint.2017.06.009, 2017.
391 Goodman, A.L., Miller, T.M., Grassian, V.H.: Heterogeneous reactions of NO_2 on NaCl and Al_2O_3 particles,
392 Journal of Vacuum Science & Technology A: Vacuum, Surfaces, and Films, 16, 2585-2590, doi:
393 10.1116/1.581386, 1998.
394 Guan, C., Li, X., Luo, Y., Huang, Z.: Heterogeneous Reaction of NO_2 on α-Al_2O_3 in the Dark and Simulated
395 Sunlight, J. Phys. Chem. A, 118, 6999-7006, doi: 10.1021/jp503017k, 2014.
396 Guo, S., Hu, M., Zamora, M.L., Peng, J., Shang, D., Zheng, J., Du, Z., Wu, Z., Shao, M., Zeng, L., Molina, M.J.,
397 Zhang, R.: Elucidating severe urban haze formation in China, Proceedings of the National Academy Sciences, 11,
398 17373-17378, doi: 10.1073/pnas.1419604111, 2014.
399 Gustafsson, R.J., Orlov, A., Griffiths, P.T., Cox, R.A., Lambert, R.M.: Reduction of NO_2 to nitrous acid on
400 illuminated titanium dioxide aerosol surfaces: implications for photocatalysis and atmospheric chemistry, Chem.
401 Commun., 0, 3936-3938, doi: 10.1039/B609005B, 2006.
402 Hems, R.F., Hsieh, J.S., Slodki, M.A., Zhou, S., Abbatt, J.P.D.: Suppression of OH Generation from the
403 Photo-Fenton Reaction in the Presence of α-Pinene Secondary Organic Aerosol Material, Environmental Science
404 & Technology Letters, 4, 439-443, doi: 10.1021/acs.estlett.7b00381, 2017.
405 Hou, X., Huang, X., Jia, F., Ai, Z., Zhao, J., Zhang, L.: Hydroxylamine Promoted Goethite Surface Fenton
406 Degradation of Organic Pollutants., Environ. Sci. Technol., 51, 5118-5126, doi: 10.1021/acs.est.6b05906, 2017.
407 Huang, R.J., Zhang, Y., Bozzetti, C., Ho, K.F., Cao, J.J.: High secondary aerosol contribution to particulate

pollution during haze events in China., Nature, 514, 218-222, doi: 10.1038/nature13774, 2014.

Langridge, J.M., Gustafsson, R.J., Griffiths, P.T., Cox, R.A., Lambert, R.M., Jones, R.L.: Solar driven nitrous acid formation on building material surfaces containing titanium dioxide: A concern for air quality in urban areas? Atmos. Environ., 43, 5128-5131, doi: 10.1016/j.atmosenv.2009.06.046, 2009.

Li, H.J., Zhu, T., Zhao, D.F., Zhang, Z.F., Chen, Z.M.: Kinetics and mechanisms of heterogeneous reaction of NO_2 on $CaCO_3$ surfaces under dry and wet conditions, Atmos. Chem. Phys., 10, 463-474, doi: org/10.5194/acp-10-463-2010, 2010.

Liu, Y., Han, C., Ma, J., Bao, X., He, H.: Influence of relative humidity on heterogeneous kinetics of NO_2 on kaolin and hematite, Phys. Chem. Chem. Phys., 17, 19424-19431, doi: 10.1039/C5CP02223A, 2015.

Ma, J., Liu, Y., He, H.: Heterogeneous reactions between NO_2 and anthracene adsorbed on SiO_2 and MgO, Atmos. Environ., 45, 917-924, doi: org/10.1016/j.atmosenv.2010.11.012, 2011.

Miller, T.M., Grassian, V.H.: Heterogeneous chemistry of NO_2 on mineral oxide particles: Spectroscopic evidence for oxide-coordinated and water-solvated surface nitrate, Geophys. Res. Lett., 25, 3835-3838, doi: org/10.1029/1998GL900011, 1998.

Monge, M.E., George, C., D Anna, B., Doussin, J., Jammoul, A., Wang, J., Eyglunent, G., Solignac, G., Daële, V., Mellouki, A.: Ozone Formation from Illuminated Titanium Dioxide Surfaces, J. Am. Chem. Soc., 132, 8234-8235, doi: 10.1021/ja1018755, 2010.

Moore, K.F., Eli Sherman, D., Reilly, J.E., Hannigan, M.P., Lee, T., Collett, J.L.: Drop size-dependent chemical composition of clouds and fogs. Part II: Relevance to interpreting the aerosol/trace gas/fog system, Atmos. Environ., 38, 1403-1415, doi: 10.1016/j.atmosenv.2003.12.014, 2004.

Nanayakkara, C.E., Jayaweera, P.M., Rubasinghege, G., Baltrusaitis, J., Grassian, V.H.: Surface Photochemistry of Adsorbed Nitrate: The Role of Adsorbed Water in the Formation of Reduced Nitrogen Species on α-Fe_2O_3 Particle Surfaces, The Journal of Physical Chemistry A, 118, 158-166, doi: 10.1021/jp409017m, 2014.

Nanayakkara, C.E., Larish, W.A., Grassian, V.H.: Titanium Dioxide Nanoparticle Surface Reactivity with Atmospheric Gases, CO_2, SO_2, and NO_2: Roles of Surface Hydroxyl Groups and Adsorbed Water in the Formation and Stability of Adsorbed Products, The Journal of Physical Chemistry C, 118, 23011-23021, doi: 10.1021/jp504402z, 2014.

Ndour, M., Anna, B.D., George, C., Ka, O., Balkanski, Y., Kleffmann, J., Stemmler, K., Ammann, M.: Photoenhanced uptake of NO_2 on mineral dust: Laboratory experiments and model simulations, Geophys. Res. Lett., 35, L5812, doi: org/10.1029/2007GL032006, 2008.

Niu, H., Li, K., Chu, B., Su, W., Li, J.: Heterogeneous Reactions between Toluene and NO_2 on Mineral Particles under Simulated Atmospheric Conditions, Environ. Sci. Technol., 51, 9596-9604, doi: 10.1021/acs.est.7b00194, 2017.

Ostaszewski, C.J., Stuart, N.M., Lesko, D.M.B., Kim, D., Lueckheide, M.J., Navea, J.G.: Effects of coadsorbed water on the heterogeneous photochemistry of nitrates adsorbed on TiO_2, The Journal of Physical Chemistry A, 122, 6360-6371, doi: 10.1021/acs.jpca.8b04979, 2018.

Schuttlefield, J., Rubasinghege, G., El-Maazawi, M., Bone, J., Grassian, V.H.: Photochemistry of Adsorbed Nitrate, J. Am. Chem. Soc., 130, 12210-12211, doi: 10.1021/jp902252s, 2008.

Shen, X.J., Sun, J.Y., Zhang, X.Y., Zhang, Y.M., Zhang, L., Che, H.C., Ma, Q.L., Yu, X.M., Yue, Y., Zhang, Y.W.: Characterization of submicron aerosols and effect on visibility during a severe haze-fog episode in Yangtze River Delta, China, Atmos. Environ., 120, 307-316, doi: 10.1016/j.atmosenv.2015.09.011, 2015.

Su, H., Cheng, Y., Oswald, R., Behrendt, T., Trebs, I.: Soil nitrite as a source of atmospheric HONO and OH radicals., Science, 333, 1616-1618, doi: 10.1126/science.1207687, 2011.

Sun, Z., Kong, L., Ding, X., Du, C., Zhao, X., Chen, J., Fu, H., Yanga, X., Cheng, T.: The effects of

acetaldehyde, glyoxal and acetic acid on the heterogeneous reaction of nitrogen dioxide on gamma-alumina, Phys. Chem. Chem. Phys., 18, 9367-9376, doi: 10.1039/C5CP05632B, 2016.

Szanyi, J., Kwak, J.H., Chimentao, R.J., Peden, C.H.F.: Effect of H_2O on the adsorption of NO_2 on γ-Al_2O_3: an in situ FTIR/MS study, The Journal of Physical Chemistry C, 111, 2661-2669, doi: 10.1021/jp066326x, 2007.

Tan, F., Jing, B., Tong, S., Ge, M.: The effects of coexisting Na_2SO_4 on heterogeneous uptake of NO_2 on $CaCO_3$ particles at various RHs, Sci. Total Environ., 586, 930-938, doi: org/10.1016/j.scitotenv.2017.02.072, 2017.

Tan, F., Tong, S., Jing, B., Hou, S., Liu, Q., Li, K., Zhang, Y., Ge, M.: Heterogeneous reactions of NO_2 with $CaCO_3$-$(NH_4)_2SO_4$ mixtures at different relative humidities, Atmos. Chem. Phys., 16, 8081-8093, doi: 10.5194/acp-16-8081-2016, 2016.

Tang, M., Huang, X., Lu, K., Ge, M., Li, Y., Cheng, P., Zhu, T., Ding, A., Zhang, Y., Gligorovski, S., Song, W., Ding, X., Bi, X., Wang, X.: Heterogeneous reactions of mineral dust aerosol: implications for tropospheric oxidation capacity, Atmos. Chem. Phys., 17, 11727-11777, doi: 10.5194/acp-17-11727-2017, 2017.

Tang, S., Ma, L., Luo, M., Zhang, Z., Cao, X., Huang, Z., Xia, R., Qiu, Y., Feng, S., Zhang, P., Xia, C., Jin, Y., Xu, D.: Heterogeneous reaction of Cl_2 and NO_2 on γ-Al_2O_3: A potential formation pathway of secondary aerosols, Atmos. Environ., 188, 25-33, doi: 10.1016/j.atmosenv.2018.06.005, 2018.

Underwood, G.M., Miller, T.M., Grassian, V.H.: Transmission FT-IR and Knudsen Cell Study of the Heterogeneous Reactivity of Gaseous Nitrogen Dioxide on Mineral Oxide Particles, The Journal of Physical Chemistry A, 103, 6184-6190, doi: 10.1021/jp991586i, 1999.

Usher, C.R., Michel, A.E., Grassian, V.H.: Reactions on mineral dust, Chem. Rev., 103, 4883-4940, doi: 10.1021/cr020657y, 2003.

Wang, L., Wang, W., Ge, M.: Heterogeneous uptake of NO_2 on soils under variable temperature and relative humidity conditions, J. Environ. Sci.-China, 24, 1759-1766, doi: org/10.1016/S1001-0742(11)61015-2, 2012.

Wang, L., Wen, L., Xu, C., Chen, J., Wang, X., Yang, L., Wang, W., Yang, X., Sui, X., Yao, L., Zhang, Q.: HONO and its potential source particulate nitrite at an urban site in North China during the cold season, Sci. Total Environ., 538, 93-101, doi: 10.1016/j.scitotenv.2015.08.032, 2015.

Wang, T., Liu, Y., Deng, Y., Fu, H., Zhang, L., Chen, J.: Adsorption of SO_2 on mineral dust particles influenced by atmospheric moisture, Atmos. Environ., 191, 153-161, doi: 10.1016/j.atmosenv.2018.08.008, 2018a.

Wang, T., Liu, Y., Deng, Y., Fu, H., Zhang, L., Chen, J.: The influence of temperature on the heterogeneous uptake of SO_2 on hematite particles, Sci. Total Environ., 644, 1493-1502, doi: 10.1016/j.scitotenv.2018.07.046, 2018b.

Wang, T., Liu, Y., Deng, Y., Fu, H., Zhang, L., Chen, J.: Emerging investigator series: heterogeneous reactions of sulfur dioxide on mineral dust nanoparticles: from single component to mixed components, Environmental Science: Nano, 5, 1821-1833, doi: 10.1039/C8EN00376A, 2018c.

Wu, L., Tong, S., Ge, M.: Heterogeneous Reaction of NO_2 on Al_2O_3: The Effect of Temperature on the Nitrite and Nitrate Formation, J. Phys. Chem. A, 117, 4937-4944, doi: 10.1021/jp402773c, 2013.

Xia, Z., Duan, X., Tao, S., Qiu, W., Liu, D., Wang, Y., Wei, S., Wang, B., Jiang, Q., Lu, B., Song, Y., Hu, X.: Pollution level, inhalation exposure and lung cancer risk of ambient atmospheric polycyclic aromatic hydrocarbons (PAHs) in Taiyuan, China, Environ. Pollut., 173, 150-156, doi: 10.1016/j.envpol.2012.10.009, 2013.

Xue, J., Yuan, Z., Griffith, S.M., Yu, X., Lau, A.K.H., Yu, J.Z.: Sulfate Formation Enhanced by a Cocktail of High NO_x, SO_2, Particulate Matter, and Droplet pH during Haze-Fog Events in Megacities in China: An Observation-Based Modeling Investigation, Environ. Sci. Technol., 50, 7325-7334, doi: 10.1021/acs.est.6b00768, 2016.

Yang, Y., Teng, F., Kan, Y., Yang, L., Liu, Z., Gu, W., Zhang, A., Hao, W., Teng, Y.: Investigation of the

charges separation and transfer behavior of BiOCl/BiF_3 heterojunction, Applied Catalysis B: Environmental, 205, 412-420, doi: 10.1016/j.apcatb.2016.12.062, 2017.

Ye, C., Zhang, N., Gao, H., Zhou, X.: Photolysis of Particulate Nitrate as a Source of HONO and NO_x, Environ. Sci. Technol., 51, 6849-6856, doi: 10.1021/acs.est.7b00387, 2017.

Ye, C., Zhou, X., Pu, D., Stutz, J., Festa, J., Spolaor, M., Tsai, C., Cantrell, C., Mauldin, R.L., Campos, T., Weinheimer, A., Hornbrook, R.S., Apel, E.C., Guenther, A., Kaser, L., Yuan, B., Karl, T., Haggerty, J., Hall, S., Ullmann, K., Smith, J.N., Ortega, J., Knote, C.: Rapid cycling of reactive nitrogen in the marine boundary layer, Nature, 532, 489-491, doi: 10.1038/nature17195, 2016.

Yu, T., Zhao, D., Song, X., Zhu, T.: NO_2-initiated multiphase oxidation of SO_2 by O_2 on $CaCO_3$ particles, Atmos. Chem. Phys., 18, 6679-6689, doi: 10.5194/acp-2017-900, 2018.

Yu, Z., Jang, M.: Simulation of heterogeneous photooxidation of SO_2 and NO_2; in the presence of Gobi Desert dust particles under ambient sunlight, Atmos. Chem. Phys., 18, 14609-14622, doi: 10.5194/acp-2018-68, 2018.

Zhang, P., Lee, J., Kang, G., Li, Y., Yang, D., Pang, B., Zhang, Y.: Disparity of nitrate and nitrite in vivo in cancer villages as compared to other areas in Huai River Basin, China, Sci. Total Environ., 612, 966-974, doi: 10.1016/j.scitotenv.2017.08.245, 2018.

Zhang, Q., Quan, J., Tie, X., Li, X., Liu, Q., Gao, Y., Zhao, D.: Effects of meteorology and secondary particle formation on visibility during heavy haze events in Beijing, China, Sci. Total Environ., 502, 578-584, doi: 10.1016/j.scitotenv.2014.09.079, 2015.

Zhang, R., Wang, G., Guo, S., Zamora, M.L., Ying, Q., Lin, Y., Wang, W., Hu, M., Wang, Y.: Formation of Urban Fine Particulate Matter, Chem. Rev., 115, 3803-3855, doi: 10.1021/acs.chemrev.5b00067, 2015.

Zhang, Z., Shang, J., Zhu, T., Li, H., Zhao, D., Liu, Y., Ye, C.: Heterogeneous reaction of NO_2 on the surface of montmorillonite particles, J. Environ. Sci.-China, 24, 1753-1758, doi: org/10.1016/S1001-0742(11)61014-0, 2012.

Zhao, D., Song, X., Zhu, T., Zhang, Z., Liu, Y.: Multiphase oxidation of SO_2 by NO_2 on $CaCO_3$ particles, Atmos. Chem. Phys., 18, 2481-2493, doi: 10.5194/acp-2017-610, 2018.

Zheng, X., Li, D., Li, X., Chen, J., Cao, C., Fang, J., Wang, J., He, Y., Zheng, Y.: Construction of ZnO/TiO_2 photonic crystal heterostructures for enhanced photocatalytic properties, Applied Catalysis B: Environmental, 168-169, 408-415, doi: 10.1016/j.apcatb.2015.01.001, 2015.